

ORIENTATIONAL MELTING OF TWO-SHELL CARBON NANOPARTICLES: MOLECULAR DYNAMICS STUDY.

*Yu. E. Lozovik, A. M. Popov**

*Institute of Spectroscopy, Russian Academy of Science, 142190,
Troitsk, Moscow region, Russia*

The energetic characteristics of two-shell carbon nanoparticles ("onions") with different shapes of second shell are calculated. The barriers of relative rotation of shells are found to be surprisingly small therefore free relative rotation of shells can take place at room temperature. The intershell orientational melting of the nanoparticle is studied by molecular dynamics. The parameters of Arrhenius formula for jump rotational intershell diffusion are calculated. The rotation of shells can be observed beginning from temperature 70 K.

I. INTRODUCTION

The discovery of fullerenes [1] and the elaboration of method of their production in arc discharge [2] gives rise the interest to another carbon nanostructures produced in arc discharge, in particular, nanoparticles with shell structure [3]. A set of works is devoted to their structure and energetics [4]– [12]. Nevertheless, an attention has not yet been given to thermodynamical properties of carbon nanoparticles with shell structure. The melting of single cluster can essentially differ from phase transitions in macroscopic systems [13]– [19]. Particularly, the melting of a mesoscopic cluster with shell structure can manifest itself as an hierarchy of rearrangements with breaking intershell orientational order and then breaking shell structure and order in particles positions inside shells. E.g., in 2D mesoscopic clusters with Coulomb [13]– [16], screened Coulomb [17], logarithmic [18] and dipole [19] interaction between particles the orientational melting (breaking the orientational order between the shells) precedes melting inside the shells.

The van der Waals interaction between atoms of neighbour shells in carbon nanoparticles is considerably weaker than chemical bonds between atoms inside the shell. So it is naturally that these nanoparticles are possible candidates for orientational melting [4]. The possibility of orientational melting of long two-shell carbon nanotube was discussed [20]. The orientational melting in carbon nanotube bundle was also theoretically studied [21].

The orientational melting can be considered as a two stage phenomenon. At low temperatures the relative orientations of shells are freezed. The intershell reorientations begin with increasing of temperature. For low temperature these reorientations occur as jumps between fixed relative shell orientations corresponding to minima of nanoparticle energy (jump rotational diffusion). For high temperature free rotation of shells take place. In the present paper the zero temperature energetic characteristics of two-shell carbon nanoparticle $C_{60}@C_{240}$ are calculated. The obtained values for barriers of relative rotations of shells are small enough to free rotation of shells take place at room temperature. The orientational melting of this nanoparticle is studied here by molecular dynamics technique.

II. SIMULATION DETAILS

The following reasons have determined our choice of nanoparticle shells. The TEM images shows that the inner shell of carbon nanoparticle can have a size that is close to the size of fullerene C_{60} [22,23]. The fullerene C_{60} with I_h symmetry is the smallest fullerene without adjacent pentagons in its structure. Fullerenes smaller than C_{60} can not be directly extracted by the use of any solvent from soot, obtained in arc discharge (see, for example, [24,25]). To explain this fact it was proposed that atoms of fullerenes which belong to two adjacent pentagons can have chemical bonds with neighbor fullerenes in soot [27]. For example, chemical bonds between all neighbour fullerenes are present in solid C_{36} [29]. Therefore we consider C_{60} as the smallest inner shell where the absence of chemical bonds between shells is very probable (it is a necessary condition for existence of relative rotation of shells). Used single and double bonds lengths of C_{60} are 1.391 Å and 1.455 Å, respectively [30]. We accept the fullerene C_{240} with I_h symmetry as outer shell of nanoparticle. This model gives the distance between shells in agreement with experiment [23] being close to the distance between graphite planes. Besides the fullerene C_{240} with I_h symmetry have greater binding energy than fullerenes C_{240} with other structures [6]. Several sets of geometric parameters corresponding to different shapes of fullerene C_{240} obtained by *ab initio* calculations of minima of binding energy [4,7,8] are used. Different shell

*Corresponding author. Fax: +7-095-334-0886; e-mail: popov@isan.troitsk.ru

shapes B , C , D and E were found by optimization of all independent geometric parameters of fullerene C_{240} with I_h symmetry. The shapes B and D corresponding to global and local minima found by York *et al* [7] that are close to sphere and truncated icosahedron respectively. The shape E corresponds to the single minimum found by Osawa [4]. It is intermediate between shapes B and D . The shape C is rather close to shapes E . It corresponds to the minimum found by Scuceria [8]. The shape A is obtained by optimization of less number of independent geometric parameters so that all atoms of this shape are arranged on the sphere [7].

We describe the interaction between atoms of neighbour shells by Lennard-Jones potential $U = 4\epsilon((\sigma/r^{12}) - (\sigma/r)^6)$ with parameters $\epsilon = 28$ K and $\sigma = 3.4$ Å. These parameters were used for the simulation of solid C_{60} [31]. The interaction between atoms inside shells we describe by Born potential:

$$U = \frac{\alpha - \beta}{2} \sum_{i,j=1}^{60} \left(\frac{(\mathbf{u}_i - \mathbf{u}_j) \mathbf{r}_{ij}}{|\mathbf{r}_{ij}|} \right)^2 + \frac{\beta}{2} \sum_{i,j=1}^{60} (\mathbf{u}_i - \mathbf{u}_j)^2 \quad (1)$$

where \mathbf{u}_i , \mathbf{u}_j are displacements of atoms from equilibrium positions, \mathbf{r}_{ij} are distances between atoms. We take $\alpha = 1.14 \cdot 10^3$ N/m and $\beta = 1.24 \cdot 10^2$ N/m. Born potential with these values of force constants gives adequate internal vibrational spectrum of C_{60} [32]. Born potential is correct only near the bottom of potential well. Nevertheless we believe that this potential is adequate for our simulation because we use it at temperatures that are one-two order of magnitude less than the temperature of fullerene destruction.

The orientational melting of nanoparticle $C_{60} @ C_{240}$ with shape D of C_{240} we studied by molecular dynamics technique. The simulations are performed in microcanonical ensemble. The equations of motion were integrated using the leap frog algorithm. We used the integration step $\tau = 6.1 \cdot 10^{-16}$ s (about one hundred steps for period of atoms vibration inside shells). Initially the system has been brought to the equilibrium during 300-500 ps that is about 30–50 librations of shells. The average fluctuations of the total energy and temperature of the system fall and flatten out during this period. Then the system was studied during 100 ps. The average fluctuations of the total energy of the system were within 0.3 % and the average fluctuations of temperature were within 1.3 %. The angular velocities of shells change rather slowly. Therefore all investigated quantities were averaged over 34-46 different realizations of the systems at the same temperature but with different energies accounting for relative rotation of shells (i.e. with different random angular velocities of shells).

III. RESULTS AND DISCUSSION

A. Ground state energetics

The global and local minima of total nanoparticle energy are found by optimization of three angles of their *relative* orientation. The total energy of nanoparticle includes the energy of interaction between shells and energy of shell deformation. We describe the relative orientations corresponding to minima of total energy in terms of three angles α_z , α_y and α_x of subsequent rotations of first shell around axes OZ, OY and OX of coordinate system. The centers of both shells coincide with the center of coordinate system. The angles α_z , α_y and α_x were measured from the initial orientation shown on Fig. 1. Due to the high I_h symmetry of shells the number of any equivalent minima (global or local) is 60. Such equivalent minima correspond to different relative orientations of shells. The energies of interaction between shells and angles of one of the orientations corresponding to global and local minima of total energy of nanoparticle are listed in Table 1.

The energies of interaction between shells calculated here are slightly less than 16.9 [9], 18.57 [10] and 20.3 [9] meV/atom obtained using another representations of van der Waals interaction and are about three times less than estimation 65.3 meV/atom for graphite [33]. Note, that the energy of total interaction between shells is not maximal for perfect sphere in comparison with other shapes of C_{240} contrary to the assumption of Lu and Yang [10].

We observed that the angles of orientations corresponding to global and local minima are determined by the shape of second shell. For the shapes C , D and E of C_{240} the initial relative orientation of shells (where symmetry axis of shells coincide) corresponds to global minima of total nanoparticle energy (note, that all these shapes of C_{240} are close to the truncated icosahedron). Several global minima for shape D are shown on Fig. 2a. One type of local minima is found for these shapes of C_{240} . For the shape B (which is close to sphere) orientations with coinciding symmetry axes correspond only to local minima (see Fig 2b). No minima correspond to such orientations for the "spherical" shape A . For "spherical" shape of C_{240} two types of local minima are found. The differences ΔE_{loc} in total nanoparticle energies between global and local minima are very small and also determined by the shape of second shell (see Table 2). These differences decrease with decreasing the average deviation $\langle \Delta R_{i2} \rangle = \langle |R_{i2} - \langle R_{i2} \rangle| \rangle$ of second shell from perfect sphere, where R_{i2} is the distance between an atom of second shell and the center of nanoparticle. The

differences ΔE_{loc} also decrease when the average distance between shells $h = \langle R_{i2} \rangle - \langle R_{i1} \rangle$ approaches to the distance r_{min} corresponding to the minimum in pair interatomic potential. This fact can be explained as follows: the change of distance d_{12} between two atoms of neighbour shells causes the less change of interaction energy between these atoms for the distances d_{12} corresponding to the bottom of interatomic potential well in comparison with the distances d_{12} corresponding to the walls of this well.

The calculated energies of shell deformation are presented in Table 2. The influence of shell deformation on the barriers of relative rotation of shells is studied as an example for barriers B_5 of shell rotation around fifth order axes of symmetry. (Barriers B_5 was calculated for the relative orientation where symmetry axes of shells have the same directions). The comparison of barriers B_5 calculated with taking into account shell deformation and without it gives the difference less than 1 % for all five shapes of C_{240} investigated here (Note that the barrier B_5 calculated here for the shape E of C_{240} is 12 % less than that obtained by Osawa used the tandem of molecular orbital and molecular mechanics calculations [4]). Therefore the shell deformations are disregarded here in calculation of barriers of relative rotation of shells, i.e. lengths of bonds angles between bonds inside shells are supposed to be fixed during intershell rotation. Note, that opposite situation take place e.g. for clusters with logarithmic interaction between particles [18]. In this case the interparticle interactions inside shell and between shells are the same and therefore the considering of shells deformation is necessary in calculation of barriers for rotation. The relative displacement of the centres of symmetry of shells causes an increase in intershell interaction energy. Therefore the common center of symmetry of both shells also supposed to be fixed during rotation.

The barriers of relative rotation of shells in the nanoparticles under consideration are calculated for relative orientations corresponding to global minima of total nanoparticle energies. It is found that the obtained values of barriers for rotation are *surprisingly small* (see Table 2). Magnitudes of these barriers are very sensitive to the shape of C_{240} and decrease when $\langle \Delta R_{i2} \rangle \rightarrow 0$ and $h \rightarrow r_{min}$ (analogously to the differences ΔE_{loc} in interaction energies between global and local minima). Moreover, these barriers are only several times greater than barriers B_a in dependencies of interaction energy between *only one atom* of the second shell and the whole first shell vs. angle of rotation. For example, for the nanoparticle with shape D of C_{240} the barrier for rotation around fifth order axis is 158.8 K. Simultaneously the maximal barrier among the barriers B_a for different atoms of the second shell is 21.6 K. The detailed analysis shows that maxima of barriers B_a for individual atoms in the same shell corresponds to *different angles* of rotation and so the dependence of total energy on angle of rotation is *essentially smoothed* (see Fig. 3). Note, that the using of spherical shape of C_{240} leads to significant underestimation of barriers for rotation.

The radii of shells of nanoparticle $C_{60} @ C_{240}$ are very close to radii of shells of (5,5)@(10,10) two-shell carbon nanotube. It is interest that barriers for relative rotation of shells per one atom calculated here for all considered nanoparticles are order of magnitude less than appropriate barrier in (5,5)@(10,10) two-shell carbon nanotube calculated by Kwon and Tomanek [20].

B. Molecular dynamics simulation

We have investigated by molecular dynamics technique the angular velocity autocorrelation function of shells, the spectrum of shell librations, the frequency of shell reorientations, distributions of Euler angles of relative orientations of shells and heat capacity of nanoparticle.

The dependence of total energy on temperature is used to calculate the heat capacity of nanoparticle. In investigated temperature region 30 – 150 K the heat capacity per one degree of freedom has no difference from the heat capacity of harmonic oscillator system within the accuracy of calculation that is less than 5 %. Only three degrees of freedom accounted for relative orientation of shells. Therefore as was to be expected there is not any peculiarities in the dependency of heat capacity on temperature and the orientational melting of two-shell carbon nanoparticle has a crossover behavior: the free rotation of shells observed in few realizations of the system at temperature 70 K and in a half realizations of the system at temperature 140 K.

The dependence of shells reorientation frequency ν vs. temperature T is shown on Fig. 4. The jump orientational intershell diffusion takes place where $kT \ll B_{re}$, B_{re} is an effective energy barrier of reorientation. The reorientation frequency ν for jump orientational intershell diffusion we interpolate at temperatures 30 – 100 K by the Arrhenius formula (thick line on Fig. 4):

$$\nu = \Omega_0 \exp \left(-\frac{B_{re}}{kT} \right), \quad (2)$$

where Ω_0 is a frequency multiplier. The fitting by least square technique gives $B_{re} = 167 \pm 22$ Kelvin degrees and $\Omega_0 = 540 \pm 180 \text{ ns}^{-1}$. The using of shorter temperature range $T = 30 - 75$ K for interpolation is found to have only a slight influence on calculated parameters B_{re} and Ω_0 .

The exponential increase of reorientation frequency ν ends at temperatures $100 - 150$ and this shows the beginning of free rotation of shells. It can be shown that the reorientation frequency ν at temperature $T \gg B_{re}$ can be estimated by the expression

$$\nu = \frac{n}{2\pi} \sqrt{\frac{3kT(I_1 + I_2)}{I_1 I_2}} \quad (3)$$

where n is an average number of reorientations over the period of relative shell rotation ($n \approx 5$), I_1 and I_2 are moments of inertia of 1-st and 2-nd shells respectively. The dependence of reorientation frequency on temperature defined by Eq. (3) is shown on Fig. 4 by thin line.

The prominent smooth of distributions of Euler angles of relative orientations of shells (Fig. 5), the disappearance of maxima in the angular velocity autocorrelation function of shells (Fig. 6) and in the spectrum of shell librations (Fig. 7) confirm that the free rotation of shells determines the thermodynamical behaviour of the nanoparticle at temperatures greater than 140.

Thus it is found that process of orientational melting for the two-shell nanoparticle occurs at temperatures that are at least 10 times less than the temperature of total melting. Analogously orientational melting can occur also in many-shell nanoparticles and short many shell nanotubes [34]. As we have shown the barriers for rotation are very sensitive to the shape of shells. Therefore, the realization of possible rotational melting in many-shell nanoparticles is determined by their shape. The nanoparticles obtained in arc discharge are faceted in shape [3,35]. However, they change their shape to almost spherical one when they are subjected to very strong electron irradiation in a high-resolution electron microscope [23,33,36]. The accurate *ab initio* calculation of geometric parameters of large shells are necessary for performance of theoretical studies of possible orientational melting of many-shell nanoparticles. Nevertheless, the theory does not provide accurate coordinates. Some works predict that many-shell nanoparticles are faceted [6,9] and some that they are spherical [10,12]. The calculations also shown that the faceted nanoparticles transform to spherical under high temperature [9,11]. Therefore the barriers for rotation may *decrease* with *increasing* of temperature due to change of shell structure.

The carbon nanoparticles with shell structure are not the single example of different types of atom interaction inside shell and between shells. A two-shell spherical nanoparticle from MoS_2 was produced [12]. We believe that orientational melting can also take place in nanoparticles from this material.

The orientational melting in a single nanoparticle may be revealed by IR or Raman study of the temperature dependence of width of spectral lines. The last must have Arrhenius-like contribution in reorientational phase (analogously to the behavior in plastic crystals, see, e.g., [37] and references herein). Moreover this study can give the estimation of reorientational barriers. Besides NMR line narrowing can be observed in reorientational phase.

ACKNOWLEDGEMENTS

This work was supported by grants of Russian Foundation of Basic Researches, Programs "Fullerenes and Atomic Clusters" and "Surface and Atomic Structures".

- [1] H.W. Kroto, J.R. Heath, S.C. O'Brien, R.F. Curl, R.E. Smalley, *Nature* 318 (1985) 162.
- [2] W. Kratschmer, L.D. Lamb, K. Fostiropoulos, D.R. Huffman, *Nature* 347 (1990) 354.
- [3] S. Iijima, *J. Crystal Growth*, 50 (1980) 675.
- [4] M. Yoshida, E. Osawa, *Ful. Sc. & Tech.* 1 (1993) 54.
- [5] D. Tomanek, W. Zhang, E. Krastev, *Phys. Rev. B* 48 (1993) 15461.
- [6] A. Maiti, C.J. Brabec, J. Bernhole, *Phys. Rev. Lett.* 70 (1993) 3023.
- [7] D. York, J.P. Lu, W. Yang, *Phys. Rev. B* 49 (1994) 8526.
- [8] G.E. Scuceria, *Chem. Phys. Lett.* 243 (1995) 193.
- [9] A. Maiti, C.J. Brabec, J. Bernhole, *Mod. Phys. Lett. B* 7 (1993) 1883.
- [10] J.P. Lu, W. Yang, *Phys. Rev. B* 49 (1994) 11421.
- [11] A. Maiti, C.J. Brabec, J. Bernhole, *Chem. Phys. Lett.* 219 (1994) 473.
- [12] D.J. Srolovita, S.A. Safran, M. Homyonfer, R. Tenne, *Phys. Rev. Lett.* 74 (1995) 1779.

- [13] Yu.E. Lozovik, *Usp. Fiz. Nauk* (in Russian) 153 (1987) 356 [*Sov. Phys. Usp.* 30 (1987) 912].
- [14] Yu.E. Lozovik, V.A. Mandelshtam, *Phys. Lett. A* 145 (1990) 269.
- [15] Yu.E. Lozovik, E.A. Rakoch, *Phys. Lett. A* 240 (1998) 311.
- [16] V.M. Bedanov, F.M. Peeters, *Phys. Rev. B* 49 (1994) 2667.
- [17] G.E. Astrakharchik, A.I. Belousov, Yu.E. Lozovik, *Phys. Lett. A* 258 (1999) 123.
- [18] Yu.E. Lozovik, E.A. Rakoch, *Phys. Rev. B* 57 (1998) 1214.
- [19] Yu.E. Lozovik, E.A. Rakoch, *Phys. Lett. A* 235 (1997) 55.
- [20] Y.K. Kwon, D. Tomanek, *Phys. Rev. B* 58 (1998) R16001.
- [21] Y.K. Kwon, D. Tomanek, *Phys. Rev. Lett.* 84 (2000) 1483.
- [22] S. Iijima, *J. Phys. Chem.* 91 (1987) 3466.
- [23] D. Ugarte, *Nature* 359 (1992) 707.
- [24] D.M. Parker, P. Wurz, K. Chatterjee, K.R.E. Lykke, J.E. Hunt, M.J. Pellin, J.C. Hemminger, D.M. Gruen, L.M. Stock, *J. Am. Chem. Soc.* 113 (1991) 7499.
- [25] Y. Chai, T. Guo, C. Jin, R.E. Haufler, L.P.F. Chibante, J. Fure, L. Wang, J.M. Alford, R.E. Smalley, *J. Phys. Chem.* 95 (1991) 7564.
- [26] Yu.E. Lozovik, A.M. Popov, *Phys. Low-Dim. Str.* 6 (1994) 33.
- [27] Yu.E. Lozovik, A.M. Popov, *Physics Uspekhi* 40 (1997) 717.
- [28] Yu.E. Lozovik, A.M. Popov, in *Physics of Clusters*, eds. G.N.Chuev and V.D.Lakhno (World Scientific Publishing, Singapore, 1998) 1-55.
- [29] C. Pishot, J. Yarger, A. Zetti, *Nature* 395 (1998) 771.
- [30] W.I.F. David, R.M. Ibbserson, J.C. Matthewman, K. Prassides, T.J.S. Dennis, J.P. Hare, H.W. Kroto, R. Taylor, D.R.M. Walton, *Nature* 353 (1991) 147.
- [31] A. Cheng, M.L. Klein, *J. Phys. Chem.* 95 (1991) 6750.
- [32] Q. Jiang, H. Xia, Z. Zhang, D. Tian, *Chem. Phys. Lett.* 191 (1991) 197.
- [33] D. Ugarte, *Europhys. Lett.* 22 (1993) 45.
- [34] Yu.E. Lozovik, to be published.
- [35] D. Ugarte, *Chem. Phys. Lett.* 198 (1992) 596.
- [36] D. Ugarte, *Chem. Phys. Lett.* 207 (1993) 473.
- [37] G.N. Zhizhin, Yu.E. Lozovik, M.A. Moskalova, A. Usmanov, *Soviet Physics-Doklady* 15 (1970) 36.

Table 1.

The energies E_{int} of interaction between shells of nanoparticle and one of the relative orientations of shells corresponding to the global and local minima of total nanoparticle energy; α_z , α_y and α_x are the angles of subsequent rotations of inner shell from initial orientation around axes OZ, OY and OX respectively.

Shape	E_{int} , (meV/atom)	α_z (in radians)	α_z (in radians)	α_x (in radians)
<i>A</i>	15.034	0.0819	0.1452	0.0540
<i>A</i>	15.033	0.2495	0.8128	-0.0081
<i>A</i>	15.032	0.6283	0.4634	0.0
<i>B</i>	15.124	0.6283	0.4634	0.0
<i>B</i>	15.101	0.0	0.0	0.0
<i>C</i>	15.180	0.0	0.0	0.0
<i>C</i>	15.098	0.6283	0.4634	0.0
<i>D</i>	13.819	0.0	0.0	0.0
<i>D</i>	13.777	0.6283	0.4634	0.0
<i>E</i>	15.166	0.0	0.0	0.0
<i>E</i>	15.061	0.6283	0.4634	0.0

Table 2.

The characteristics of second shell shape: the average deviation of second shell from perfect sphere $\langle \Delta R_{i2} \rangle$ and the difference between average intershell distance h and the distance r_{min} corresponding to the minimum in pair interparticle potential $l = h - r_{min}$; the differences ΔE_{loc} in total energies of nanoparticle between global and local minima; the minimal and average barriers for rotation B_{min} , $B_{av} \pm \Delta B_{av}$ respectively, where the barrier B_{av} is averaged over all directions of rotation axis and ΔB_{av} is its dispersion; the average energies of shell deformation $E_{d1} \pm \Delta E_{d1}$ and $E_{d2} \pm \Delta E_{d2}$ for first and second shells respectively, where the energies E_{d1} and E_{d2} are averaged over all relative orientations of shells and ΔE_{d1} and ΔE_{d2} are their dispersions.

Shape $\langle \Delta R_{i2} \rangle$	l (\AA)	ΔE_{loc} ($\text{^{\circ}K}$)	B_{min} ($\text{^{\circ}K}$)	$B_{av} \pm \Delta B_{av}$ ($\text{^{\circ}K}$)	$E_{d1} \pm \Delta E_{d1}$ ($\text{^{\circ}K}$)	$E_{d2} \pm \Delta E_{d2}$ ($\text{^{\circ}K}$)
<i>A</i>	-0.245	0.0	3.2; 5.5	19.0	20.5 ± 0.8	2.09 ± 0.02
<i>B</i>	-0.258	0.057	76.7	82.9	122.1 ± 12.1	1.62 ± 0.07
<i>C</i>	-0.289	0.152	287.4	349.3	363.1 ± 8.8	2.17 ± 0.26
<i>D</i>	-0.119	0.244	144.4	160.3	177.3 ± 9.6	3.75 ± 0.20
<i>E</i>	-0.299	0.147	368.3	441.2	459.9 ± 12.9	4.58 ± 0.44
						13.78 ± 0.38

Captions for illustrations.

Fig. 1. The fragments of two shells (shape D of second shell) at their initial orientations. OX, OY and OZ are axes of coordinate system. One fivefold axis of each shell is aligned with the axis OZ. One of the closest to axis OZ atoms of first and second shells (shown by black circles) lie in plane OXZ. This fixes the orientation of axes OX and OY.

Fig. 2. The dependencies of binding energies for interaction between shells of nanoparticle on their relative orientation. α_z and α_y are the angles of subsequent rotations of inner shell from initial orientation around axes Z and Y respectively. The angle of rotation around axis X is fixed equal to zero. a) shape D of second shell; b) shape B of second shell;

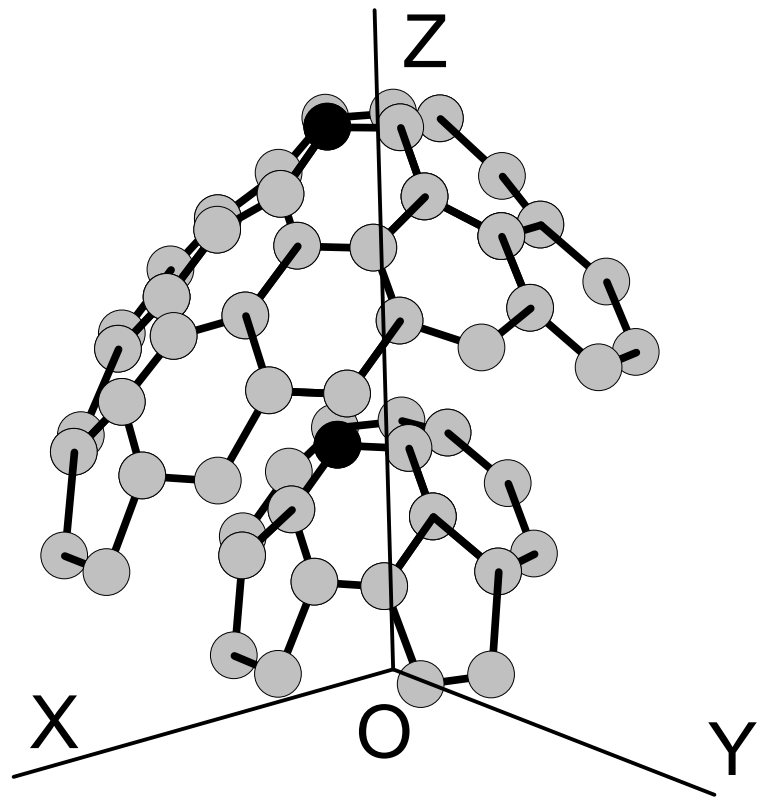
Fig. 3. Interaction energies between first shell of nanoparticle and groups of atoms of second shell with shape D vs. angle α_z of rotation of inner shell from initial orientation around axis Z. An each group include all atoms with the same dependencies of interaction energy E_a between this atom and the first shell on angle of rotation. The curves corresponding to all 25 groups of atoms with different dependencies E_a for individual atom are shown by thin lines (23 groups from 10 atoms and 2 groups from 5 atoms). The dependence of total interaction energy between shells on angle α_z is shown by bold line. All energies are measured from their minima.

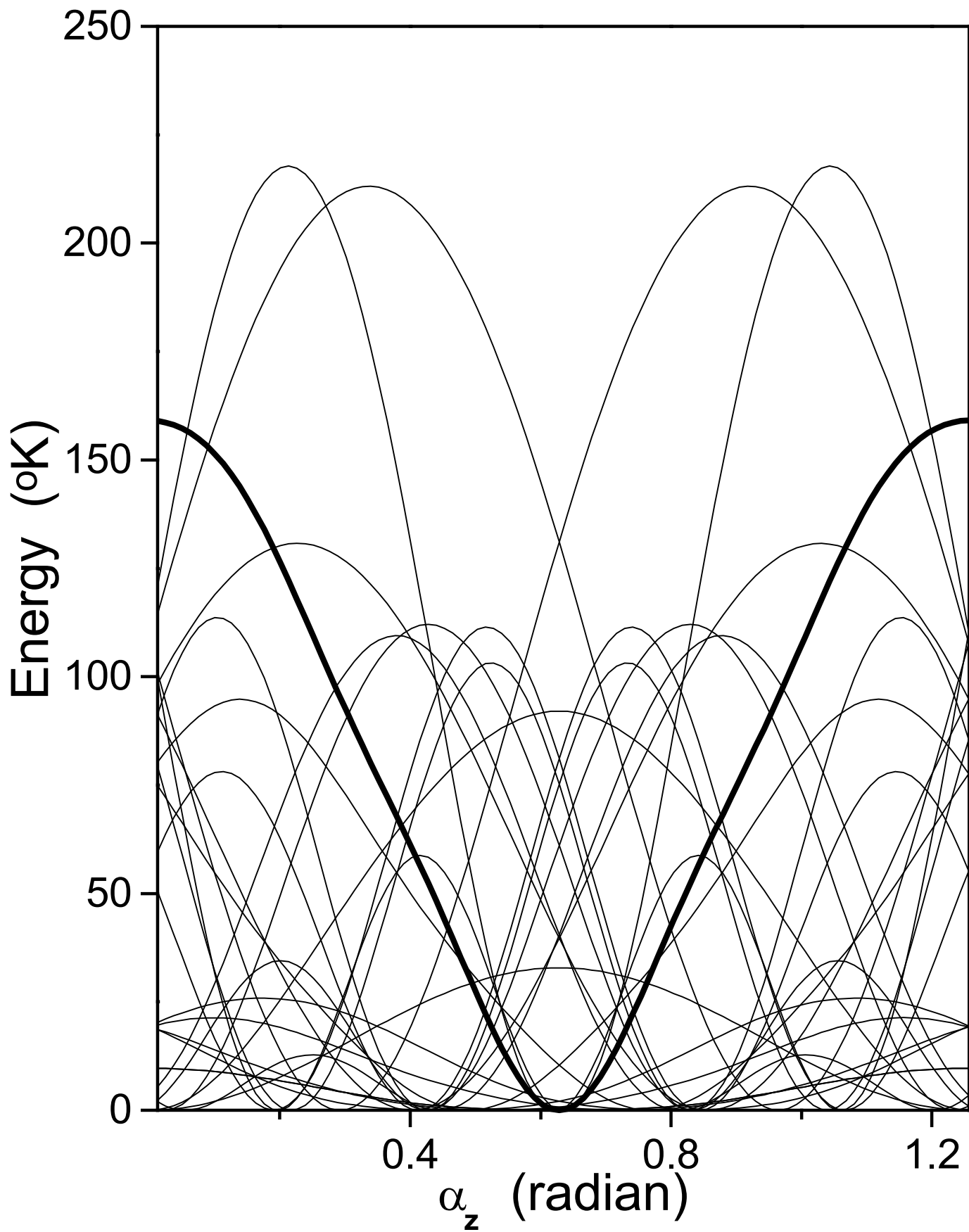
Fig. 4 The dependence of shells reorientation frequency ν on temperature T in Kelvin degrees. The interpolation by the Arrhenius formula at $T < B_{re}$ is shown by thick line. The estimation at $T > B_{re}$ is shown by thin line.

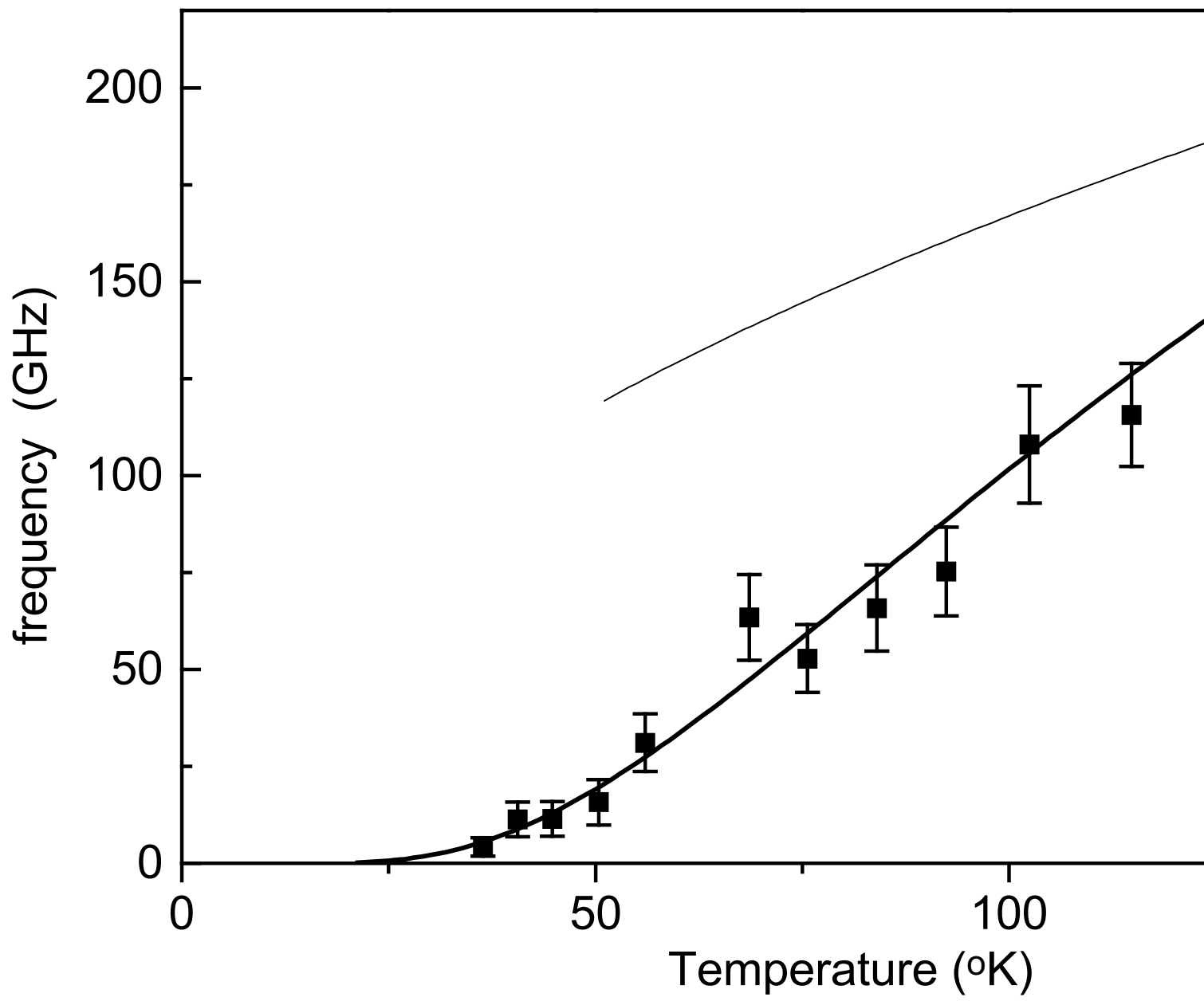
Fig. 5 The distributions of Euler angles θ , ψ and ϕ of relative orientations of shells at temperatures 21 K, 36 K and 140 K are shown by dotted lines, thin lines and thick lines respectively; a) the distribution of angle ϕ ; b) the distribution of angle θ ; c) the distribution of angle ψ .

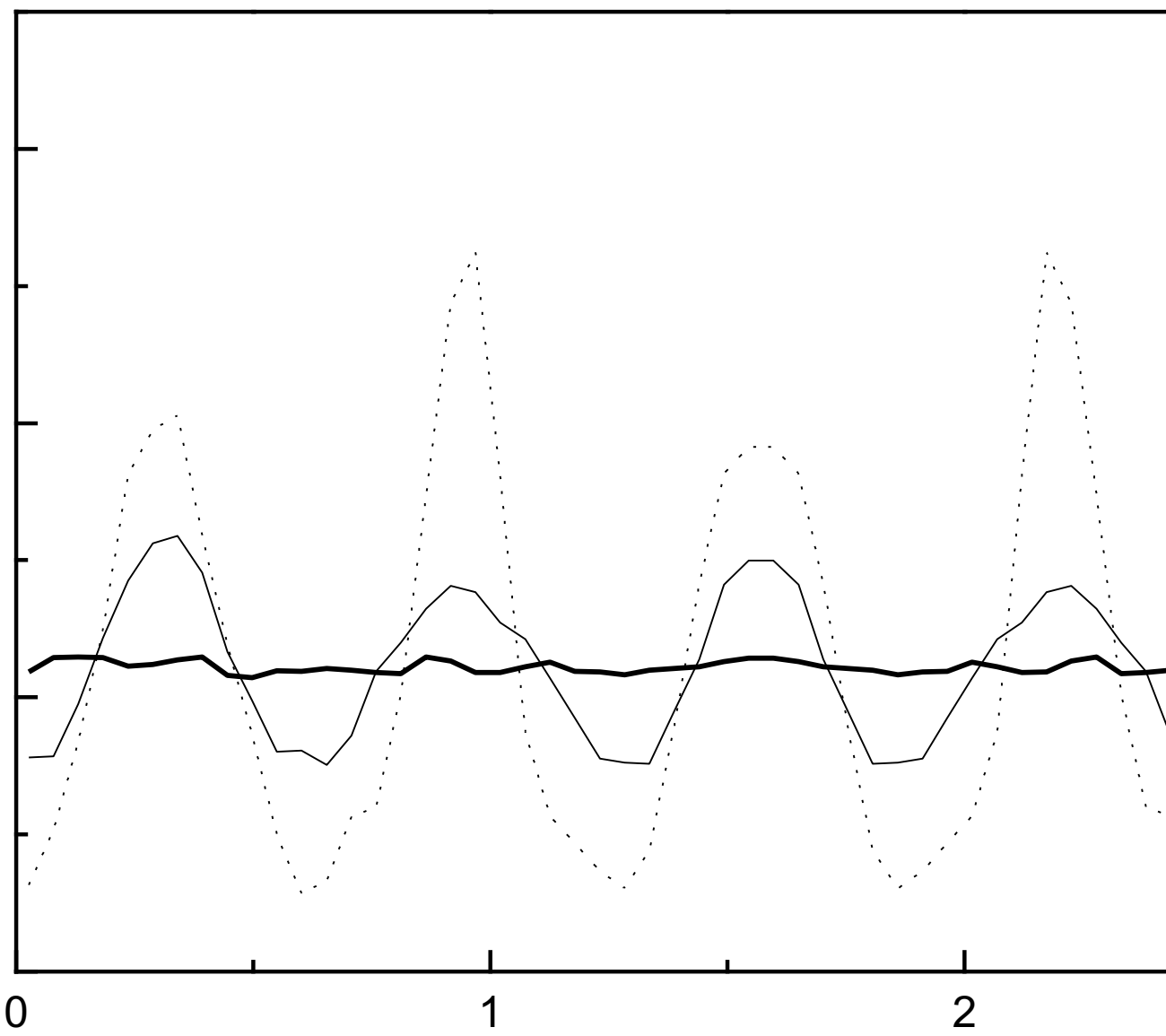
Fig. 6 The angular velocity of autocorrelation function of the first shell at temperatures 21 K, 36 K and 140 K are shown by dotted lines, thin lines and thick lines respectively.

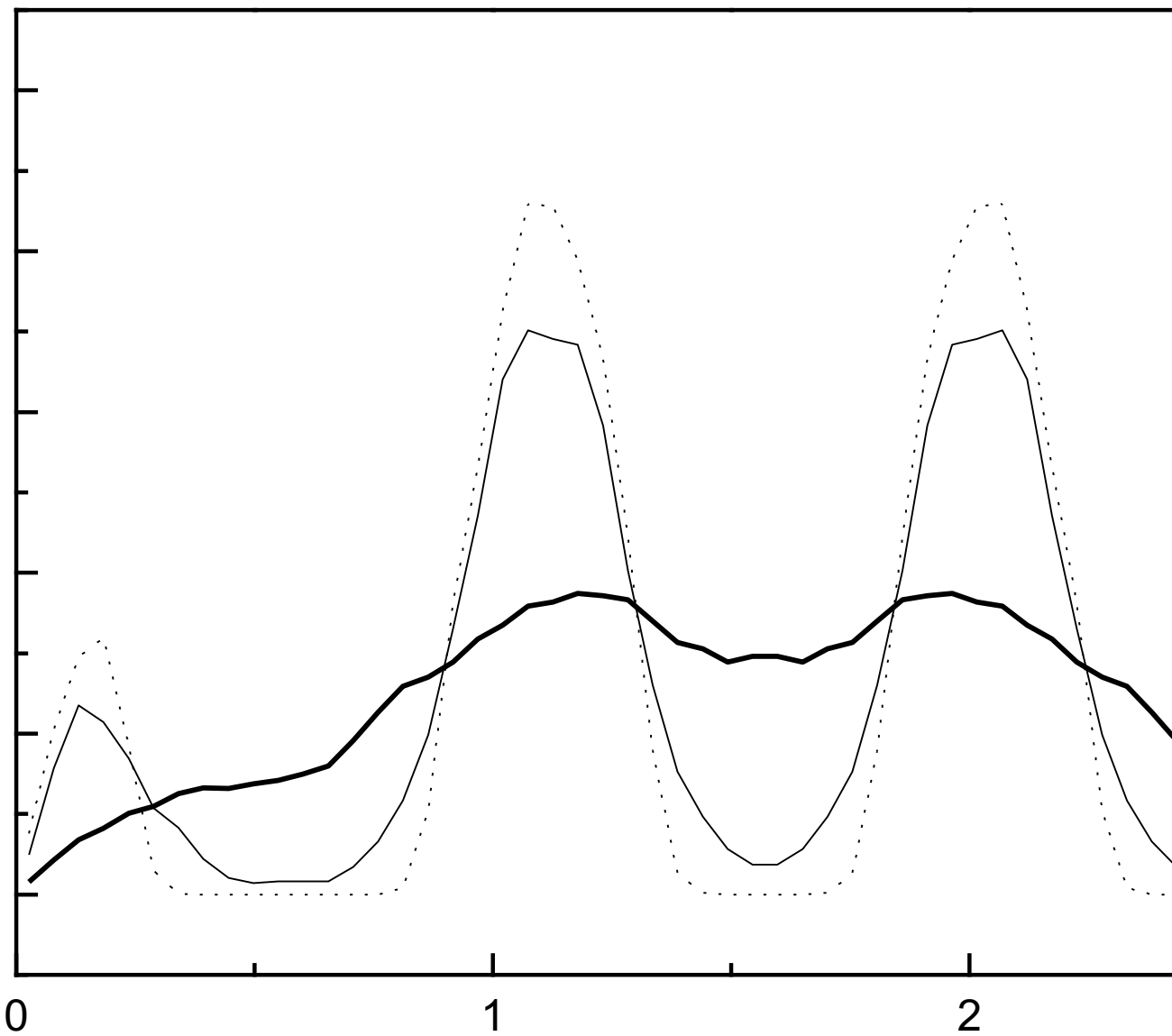
Fig. 7 The spectrum of shell librations at temperatures 21 K, 36 K and 140 K are shown by dotted lines, thin lines and thick lines respectively.

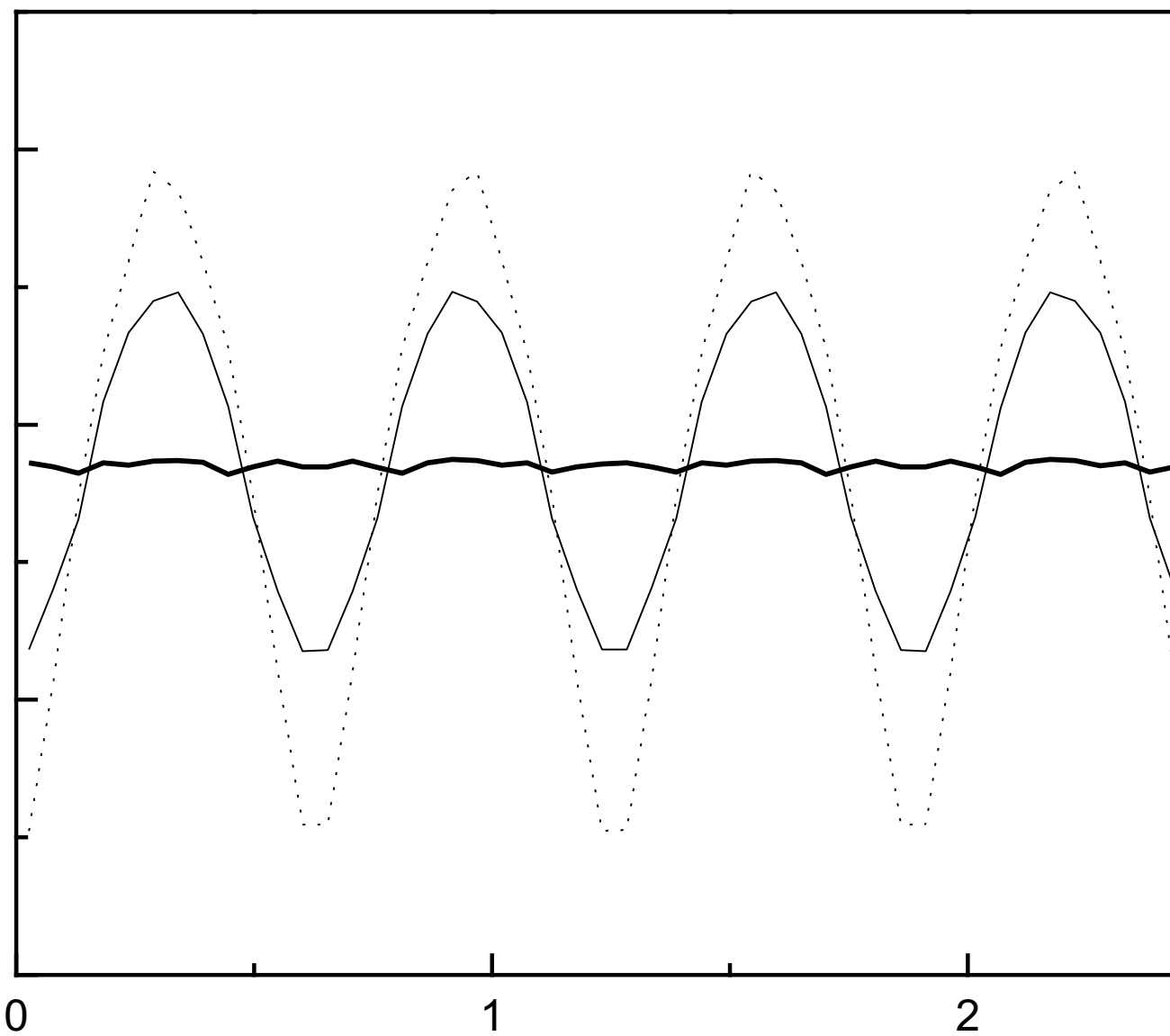












angular velocity autocorrelation function

